

The ‘Cheerios effect’

Dominic Vella and L. Mahadevan*

*Division of Engineering and Applied Sciences, Harvard University,
Pierce Hall, 29 Oxford Street, Cambridge MA 02138*

Objects that float at the interface between a liquid and a gas interact because of interfacial deformation and the effect of gravity. We discuss the mechanism behind this interaction as well as the physical conditions that lead to mutual attraction or repulsion. After outlining the method of Chan *et al.* (*J. Colloid Interface Sci.* **79** 410-418 (1981)) to quantify the force of interaction in some particular instances, we use the results to formulate a simple dynamical model of this interaction. The results obtained from this model are then validated by comparison to experimental results for the mutual attraction of two identical spheres. We conclude by looking at some of the applications of the effect that can be found in the natural and manmade worlds.

I. INTRODUCTION

Bubbles trapped at the interface between a liquid and a gas rarely rest. Over a timescale of several seconds to minutes, long-lived bubbles will be observed to move towards one another and, when contained, tend to drift towards the exterior walls - as shown in fig. 1. The sceptical reader may readily verify these claims by pouring themselves a glass of sparkling water (or, if they prefer, wine) and following the motion of those bubbles at the surface - particularly those at the periphery of the glass. This phenomenon has even been affectionately dubbed the ‘Cheerios effect’ after the observation that breakfast cereals floating in milk often clump together or stick to the walls of the breakfast bowl¹.

In this article, we bring together a number of perspectives on the Cheerios effect gathered from the literature and our own experience of probing this effect at home, in the kitchen, and in the laboratory. We show how simple physical ideas lead to an understanding not only of the attraction itself, but also of its dynamical consequences. Despite being a subject with enormous potential for simple, reliable party tricks, the technological implications of the Cheerios effect are far from frivolous. Indeed, much research is currently being undertaken to investigate the possibility of using surface tension to induce the ‘self-assembly’ of small-scale structures². Understand-



FIG. 1: Bubbles floating on water in a petri dish. The bubbles are observed to aggregate before moving to the wall of the container. After sufficiently long times, the island of bubbles in the centre also migrates to the wall.

ing the way in which particles aggregate at an interface and thence being able to control the form of the aggregate as well as the dynamics of its formation may one day enable much simplified manufacture of components of micro-electromechanical systems (MEMS).

For floating objects in equilibrium or motion, we must consider the balance of linear momentum both in the flotation plane as well as out of the plane, and in addition the balance of angular momentum in all three directions. Many of the misconceptions in the field arise from considering only some but not all of these balance equations. In the sections that follow, we focus on a series of simple examples that look at the consequences of force and torque balance by highlighting their roles in particular phenomena. We first consider the mechanism of attraction and repulsion between isotropic floating objects. We then turn to dynamical consequences of these forces, and a description of how considerations of torque balance can lead to amphiphilic strips. We conclude with some possible biological implications of our observations.

II. THE PHYSICAL ORIGIN OF ATTRACTION

The mechanism behind the apparent attraction between bubbles or between a bubble and the wall of a glass is easy to understand by considering the geometry of the interface at which the bubbles are trapped. For simplicity, we consider the latter case (schematically illustrated in fig. 2), although the explanation of the clustering of many bubbles is similar. Here, the air-water interface is significantly distorted by the presence of the wall (the well-known meniscus effect) and, since the bubble is positively buoyant, there is a net upward force, F_g , on the bubble. Because it is constrained to lie at the interface, however, the bubble cannot simply rise vertically and instead does the next best thing: to move upwards *along* the meniscus. As glass is in general wetting (the contact angle, defined in fig. 2, satisfies $\theta < \pi/2$), in moving upwards along the meniscus the bubble also moves closer to the wall. Viewed from above, it appears as if there is an exotic attractive force acting between the wall and the bubble when in fact the bubble is merely obeying gravity and moving in a constrained path imposed by the

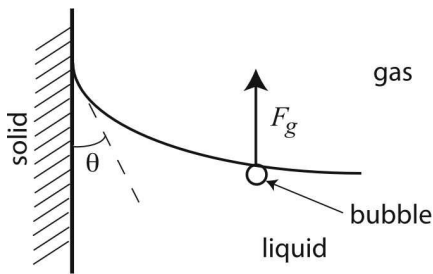


FIG. 2: Schematic of a single bubble close to a wall, along with the definition of the contact angle.



FIG. 3: A photograph of a drawing pin floating upturned on water. Notice that the deformation of the interface in this case is the opposite to that around a bubble or near a wetting wall.

presence of the wall.

Now, a single bubble will deform the interface just as the presence of a wall does, though this time for a different reason and to a lesser extent. In the bubble's case, it can only remain at the interface because the buoyancy force (that is tending to push the bubble out of the liquid) is counterbalanced by the surface tension force (that opposes the deformation of the interface and hence is tending to keep the bubble in the liquid). These two competing effects reach a compromise where the bubble is partially out of the liquid but the interface is slightly deformed. This deformation is significant enough to influence other bubbles nearby, which move 'upwards' along the meniscus, and so spontaneously aggregate.

This mechanism was first given by Nicolson³ as a means by which the bubbles that constitute a bubble raft interact and give the raft its solid-like properties. Nicolson's explanation, however, goes against the currently accepted wisdom on the cause of the Cheerios effect, which we shall give in section IV. We shall show in section V that the mechanism outlined above is certainly the dominant contribution for sufficiently small particles.

Precisely the same argument works in the case of particles that are significantly more dense than water floating at an interface. That such heavy particles can float at all is due to the fact that this time surface tension stops the interface from deforming too much *downwards* as would happen if the particle were to sink. This re-

versal of the interfacial curvature can be seen clearly in fig. 3 for a metal drawing pin floating on water: surface tension must act upwards to counterbalance the weight of the pin. By analogy with what is observed with bubbles, we should expect that another drawing pin floating near the first will 'fall' down the interface and hence the two appear to be attracted to one another - as is indeed observed.

III. REPULSION: OFTEN MISUNDERSTOOD

So far we have seen only that the deformation of an interface caused by the presence of particles at that interface can lead to mutual attraction between those particles and eventually to the formation of large clusters. This, however, is only one half of the story. Imagine that we were to float a buoyant bubble in the vicinity of a drawing pin - should they also attract? On the basis of the, by now familiar, physical argument, we expect that the bubble will move upwards along the meniscus distorted by the presence of the drawing pin. However, since the pin is not buoyant (i.e. the interface has the curvature shown in fig. 3), moving along the interface will, in this case, cause the bubble to move away from the drawing pin and so the two objects in fact *repel* one another.

A more striking demonstration of this repulsion can be achieved using two drawing pins, provided they are the kind that has a thin plastic cap around the blunt end. As we should expect from the discussion given in section II, these two drawing pins will attract when floated at the interface. However, if we now carefully remove the plastic cap from the top of one and float it (the cap) near the intact drawing pin, then the two will be seen to move apart.

This simple experiment apparently challenges the common assumption that the attraction or repulsion of particles at interfaces should depend solely on the wetting properties, namely the contact angles, of the particles (see, for example, p. 70, ex. 3 of Batchelor's book⁴ or Campbell *et al.*⁵). Here, the wetting properties of the plastic cap (which is the only part that is in contact with the liquid) are not altered by removing it from the pin but the weight that it must support is much reduced, making the cap buoyant. In turn, this alters the balance between surface tension and gravity so that the interface must now pull down on the cap to keep it at the interface and so the deformation near the cap resembles that around a bubble. This change in the sign of the curvature of the interface has been brought about without changing the surface properties of the cap, simply because of a change in the effective density of the particle: a possibility with many potential applications that appear not to have been explored fully.

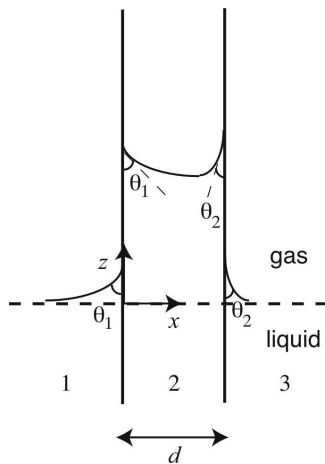


FIG. 4: The geometry of two infinite plates in a semi-infinite fluid. The planes have contact angles θ_1 and θ_2 respectively and are a horizontal distance d apart.

IV. A MODEL CALCULATION

Quantifying the physical picture outlined in section II allows us not only to predict the particle mass at which the interfacial curvature changes sign, but also to understand at a simple level the dynamical interaction between two particles. To introduce these ideas, we first consider an idealisation: calculating the force between two infinite vertical plates at a liquid-gas interface, as shown in fig. 4. This set-up is often used as a model for explaining the Cheerios effect¹ and while we argue later that this picture is incorrect for floating objects, it does lend itself to a simple calculation (for a further simplification leading to similar conclusions, the reader is referred to Maxwell⁶).

The equation of the interface $z = h(x)$ is determined from the condition that the pressure change across the interface due to surface tension (which is proportional to the curvature of the interface) is equal to the hydrostatic pressure difference caused by the deformation of the interface (see p. 65 of Batchelor⁴ for a thorough discussion of this). For small interfacial deflections, this balance may be written as:

$$\gamma \frac{d^2 h}{dx^2} = \rho g h \quad (1)$$

where γ is the surface tension coefficient of the liquid-gas interface, ρ is the density of the liquid and g is the acceleration due to gravity. Equation (1) is to be solved with the boundary conditions that the contact angles θ_1 and θ_2 are given at each of the plates and that the deflection of the interface should decay far away from the plates. In each of the regions labelled $i = 1, 2, 3$ in fig. 4, the solution of (1) gives the equation of the interface to be $z = h_i(x) = A_i e^{-x/L_c} + B_i e^{x/L_c}$ where $L_c \equiv \sqrt{\gamma/\rho g}$ is the *capillary length*, which defines the length-scale over which interactions occur. The conditions $h_1(-\infty) = 0 =$

$h_3(\infty)$ give $A_1 = 0 = B_3$, which, combined with the contact angle conditions $h'_1(0) = \cot \theta_1$ and $h'_3(d) = -\cot \theta_2$, give the interface shape outside the plates as:

$$\frac{h_1(x)}{L_c} = \cot \theta_1 e^{x/L_c} \quad (2)$$

$$\frac{h_3(x)}{L_c} = \cot \theta_2 e^{(d-x)/L_c} \quad (3)$$

while the contact angle conditions $h'_2(0) = -\cot \theta_1$ and $h'_2(d) = \cot \theta_2$ give the interface shape between the two plates to be:

$$\frac{h_2(x)}{L_c} = \frac{\cot \theta_1 \cosh\left(\frac{d-x}{L_c}\right) + \cot \theta_2 \cosh(x/L_c)}{\sinh(d/L_c)} \quad (4)$$

These expressions give the deformation of the interface from its natural state at $z = 0$. Because of this deformation, the plates are now subjected to a capillary pressure that results in a horizontal force on the plates (there is no resultant horizontal surface tension force because its components on either side of a plate cancel exactly). This force may act either to bring them together or to pull them apart depending on the two contact angles θ_1 and θ_2 . The value of the horizontal force per unit length, F_h , can be calculated by integrating the hydrostatic pressure along each of the wetted sides of one of the plates (say the one on the left in fig. 4) and taking the difference as follows:

$$\begin{aligned} F_h &= - \int_{-\infty}^{h_2(0)} \rho g z dz + \int_{-\infty}^{h_1(0)} \rho g z dz = \int_{h_2(0)}^{h_1(0)} \rho g z dz \\ &= \frac{1}{2} \rho g (h_1(0)^2 - h_2(0)^2) \end{aligned} \quad (5)$$

so that we have:

$$F_h = -\frac{\gamma}{2} \left(\frac{(\cot \theta_1 \cosh(d/L_c) + \cot \theta_2)^2}{\sinh^2(d/L_c)} - \cot^2 \theta_1 \right) \quad (6)$$

where the sign convention is such that $F_h < 0$ corresponds to attraction between the plates. Typically this force is either attractive for all plate separations or repulsive at large separations and attractive at short separations (with an unstable equilibrium at an intermediate distance). An example of a force-displacement curve in the latter case is shown in fig. 5. Equation (6) can be used to show that repulsion is possible only if $\cot \theta_1 \cot \theta_2 < 0$, i.e. if one plate is wetting and the other non-wetting, as follows. First, we note that, provided that $\cot \theta_1 \neq -\cot \theta_2$, the fact that $F_h \rightarrow 0$ as $d \rightarrow \infty$ implies that repulsion can only occur if F_h has a maximum value somewhere, since as $d \rightarrow 0$, $F_h \rightarrow -\infty$. A simple calculation shows that the only turning point of the function $f(\xi) = (\cot \theta_1 \cosh \xi + \cot \theta_2) / \sinh \xi$ occurs at $\xi = \xi^*$ where $\cosh \xi^* = -\cot \theta_2 / \cot \theta_1$, which only has a real solution ξ^* provided that $\cot \theta_1 \cot \theta_2 < 0$. When $\cot \theta_1 = -\cot \theta_2$, the short range attraction does

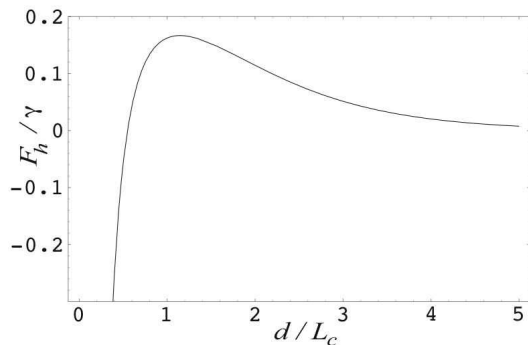


FIG. 5: A typical force-separation curve for a wetting and non-wetting plate and a liquid-gas interface. Here, $\theta_1 = 2\pi/3$ and $\theta_2 = \pi/4$ and we observe repulsion at large separations as well as attraction at short range.

not exist and instead there is repulsion at *all* displacements, but the result that repulsion can only occur when $\cot \theta_1 \cot \theta_2 < 0$ still stands.

The result just derived shows that vertical plates at a liquid-gas interface will attract if they have like menisci and repel otherwise, as we saw in section II with floating objects. However, the physical mechanism here is subtly different. We can no longer argue in terms of one plate following the meniscus imposed by the other as these plates do not float, meaning that there is no analogue of the condition of vertical force balance in this scenario. Instead, we must consider the effects of hydrostatic pressure that result from the deformation of the interface, as is detailed by Poynting and Thomson⁷. Here, we give an abbreviated version of their argument.

This explanation starts with consideration of the configurations shown in fig. 6 (a) and (b) in which plates of like wettability are at the interface. In (a), the upper portion of the central column of fluid is at a pressure lower than atmospheric pressure, p_{atm} , because of the curvature of the interface and the two plates attract because of the excess of atmospheric pressure. Similarly in (b), the pressure in the outer fluid is greater than p_{atm} , again because of the sign of the interfacial curvature, and so there is an excess pressure causing the two plates to attract. The situation is more complicated when one plate is wetting and the other non-wetting. At intermediate and large displacements, the interfacial displacement of the central column at the points where it touches a plate is *lower* than it is on the other side of the same plate (as shown in fig. 6 (c)) due to the constraint that the central interface must pass through $z = 0$ (rather than just asymptoting to 0) to allow it to satisfy both contact angle conditions. From (5), this is enough to show that the two plates repel. When the two plates come close to contact, however, it is not possible for the interface to satisfy the contact angle conditions with such small vertical displacements and so the displacement at the plates must increase, reversing the sign of the force and leading to attraction (see fig. 6 (d)). The exception to this is the

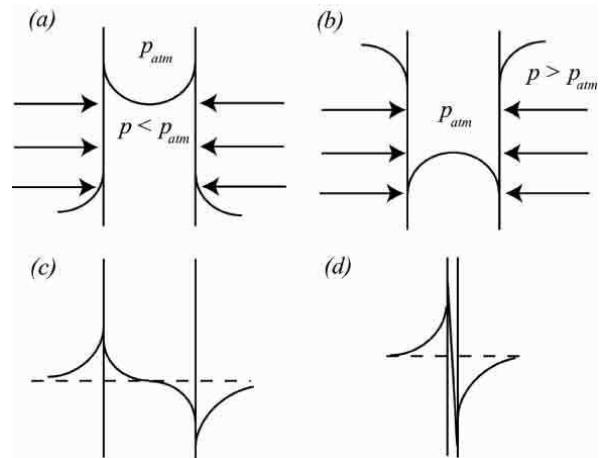


FIG. 6: Typical meniscus profiles for the different configurations of plate wettabilities. (a) Two wetting plates. (b) Two non-wetting plates. (c) A wetting and non-wetting plate at intermediate separation. (d) A wetting and non-wetting plate at short range.

case where $\cot \theta_1 = -\cot \theta_2$, as noted in the discussion following (6). Here, the interface is anti-symmetric about the centre-line of the system, i.e. $h(d/2) = 0$. Thus, the interfacial displacement of the inside of the plates is lower in magnitude than that on the outside of the plates and so, again using (5), we see mutual repulsion between the two plates, regardless of the displacement between the two plates.

The type of argument just given has often been invoked to explain the Cheerios effect (see, for example, the answer to problem 3.100 of Walker's book¹ or perform a Google search on 'Cheerios effect'). While the effects of hydrostatic pressure imbalances caused by interfacial deformation are certainly important, the calculation considered in this section cannot constitute a complete explanation since it neglects the crucial fact that Cheerios, and other floating objects, must satisfy a vertical force balance to be able to float. For small particles, this changes the physics fundamentally so that it is the picture outlined in section II that is the dominant effect. To see this, however, requires a slightly more involved calculation, which we shall now embark upon.

V. THE CASE OF FLOATING OBJECTS

Having seen the manner in which the force between two interfacial objects can be calculated in a somewhat artificial geometry, we are now in a position to consider the scenario that is of most interest to us here: interactions between objects that are *floating* at a liquid-gas interface. The major difference between this and what has gone before is that we must now take into account the vertical force equilibrium of the object. This is actually a significant enough complication that, even using the linearised approach of section IV, progress can only be made

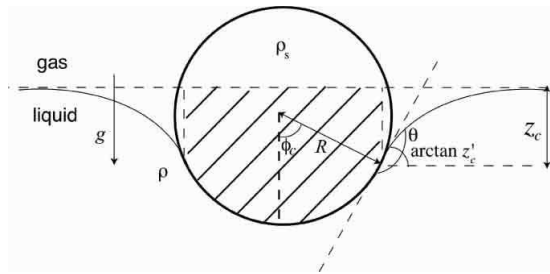


FIG. 7: Geometry of a sphere lying horizontally at a liquid-gas interface. The shaded area represents the weight of liquid equivalent to the buoyancy force due to hydrostatic pressure acting on the sphere⁹.

numerically. However, for sufficiently small particles we may assume in addition that the interfacial profiles generated by one or more object floating at the interface are sufficiently small that they may be superposed and so make progress analytically.

This assumption was tacitly made in our discussion of the attraction and repulsion of objects at interfaces in section II, but was first introduced by Nicolson³ who used it to calculate the interaction force between neighbouring bubbles in bubble rafts. It was then applied to the calculation of the force between floating particles at an interface by Chan *et al.*⁸ who considered some simple illustrative particle configurations such as two horizontal cylinders floating near one another. Here we give their argument applied to the problem of determining the interaction between two identical spheres floating at an interface.

In the spirit of the Nicolson approximation, we first neglect the presence of the second sphere and consider the vertical force balance on an isolated sphere to determine an approximate expression for the interfacial slope at the contact point, z'_c (see fig. 7). This is equivalent to determining the value of ϕ_c , as defined in fig. 7, because of the geometrical relation $\phi_c = \pi - \theta + \arctan z'_c$, but the calculation of z'_c will prove useful to justify Nicolson's approximation and to compare the results with those of section IV.

For this sphere to remain at the interface, its weight, $\frac{4}{3}\pi\rho_s g R^3$ must be balanced by the component of surface tension acting along the (circular) contact line and the buoyancy force because of the displaced bulk fluid. The first of these is easily seen to be given by $2\pi R \sin \phi_c \gamma \sin(\arctan z'_c) = 2\pi\gamma R \sin \phi_c z'_c (1 + z'^2_c)^{-1/2}$, while the second is just given by the weight of water that *would* occupy the area between the wetted region of the sphere and the undisturbed interface, which is shown as the hatched area in fig. 7 (Keller⁹ and Mansfield *et al.*¹⁰ give elegant derivations of this generalisation of Archimedes principle). This volume can be calculated by splitting the hatched volume into a circular cylinder of radius $R \sin \phi_c$ and height z_c and a spherical cap of height $R(1 - \cos \phi_c)$ and base $R \sin \phi_c$. This gives the

buoyancy force to be:

$$\pi \rho g R^3 \left(\frac{z_c}{R} \sin \phi_c + \frac{2}{3} - \cos \phi_c + \frac{1}{3} \cos^3 \phi_c \right)$$

The balance of these vertical forces may now be written explicitly as:

$$\frac{4}{3}\pi\rho_s g R^3 = 2\pi\gamma R \sin \phi_c \frac{z'_c}{\sqrt{1 + z'^2_c}} + \rho g \pi R^3 \left(\frac{z_c}{R} \sin \phi_c + \frac{2}{3} - \cos \phi_c + \frac{1}{3} \cos^3 \phi_c \right)$$

By substituting $\phi_c = \pi - \theta + \arctan z'_c$ and keeping only those terms linear in z'_c we obtain an expression for $z'_c \sin \phi_c$ accurate to linear order in the *Bond number*, $B \equiv R^2/L_c^2$:

$$z'_c \sin \phi_c = B \left(\frac{2D - 1}{3} - \frac{1}{2} \cos \theta + \frac{1}{6} \cos^3 \theta \right) \equiv B \Sigma \quad (7)$$

where $D \equiv \rho_s/\rho$. (As a consistency check, observe that $z'_c = 0$ when $\theta = \pi/2$ and $D = 1/2$, as we expect since in this case, the Archimedes buoyancy alone is enough to balance the weight of the sphere without any interfacial deformation.)

The expression for the slope of the interface in the vicinity of the spherical particle given in (7) shows that the deformation of the interface is small provided that $B \ll 1$, corresponding to a radius of ~ 1 mm or smaller for a sphere at an air-water interface. In this situation, the energy of interaction of two spheres is given by the gravitational energy of one sphere displaced vertically by the deformation of the interface imposed by the presence of a second sphere a distance l away. To calculate the energy of interaction we must therefore calculate the interfacial displacement caused by a floating sphere, which is determined by the hydrostatic balance $\gamma \nabla^2 h = \rho g h$ - the co-ordinate invariant statement of equation (1). With the assumption of cylindrical symmetry, this becomes:

$$\frac{1}{r} \frac{d}{dr} \left(r \frac{dh}{dr} \right) = \frac{h}{L_c^2} \quad (8)$$

with the boundary conditions that $h \rightarrow 0$ as $r \rightarrow \infty$ and $h'(r = R \sin \phi_c) = z'_c$. This has a solution in terms of modified Bessel functions of the first kind¹¹ and of order i , $K_i(x)$:

$$h(r) = -z'_c L_c \frac{K_0(r/L_c)}{K_1(R \sin \phi_c/L_c)} \approx -z'_c \sin \phi_c R K_0(r/L_c) \quad (9)$$

where we have used the asymptotic result (see, for example, Abramowitz and Stegun¹¹) that $K_1(x) \approx 1/x$ for $x \ll 1$ to simplify the prefactor.

The energy of interaction between the spheres is given, to leading order in B , by the product of the resultant weight of one sphere and the vertical displacement it suffers due to the presence of the other. From the vertical force balance leading to (7), we note that the resultant weight of the sphere is simply given to first order by

$2\pi R\gamma(z'_c \sin \phi_c) = 2\pi R\gamma B\Sigma$, with Σ as defined in equation (7). We may therefore write the energy, $E(l)$, as:

$$E(l) = -2\pi\gamma R^2 B^2 \Sigma^2 K_0 \left(\frac{l}{L_c} \right) \quad (10)$$

and from this, the force of interaction is given by $F(l) = -\frac{dE}{dl}$ or:

$$F(l) = -2\pi\gamma R B^{5/2} \Sigma^2 K_1 \left(\frac{l}{L_c} \right) \quad (11)$$

In the next section, we shall use the expression in (11) and see that this leads to theoretical predictions that are in reasonable agreement with experiment. However, it is important to emphasise that the calculation that led to (10) relied on a number of assumptions. The first of these is that the particle be small enough that the interfacial deformations it causes are small enough to be superposed on those of other particles (by comparison with numerical results, Chan *et al.*⁸ show that the expression derived by their method is essentially exact for Bond numbers $B \leq 0.1$).

In the calculation leading to (10), we have also neglected the effect of capillary pressure acting on the particle to produce a horizontal force - the effect whose magnitude for two vertical plates we calculated in section IV. It is not possible using the analysis presented here to include this effect since inherent in the Nicolson approximation is the assumption that the level of the interface is the same on either side of the particle. However, the difference in interface heights on either side of the sphere only occurs at the next order in B and so, using (6), we see that the contribution from capillary pressure also only enters at the next order in B without doing the detailed calculation. Thus, for small particles ($B \ll 1$) at least, Nicolson's idea that the particles obey gravity but are constrained to follow a deformed interface leads to the aggregation phenomenon, or Cheerios effect, rather than the resultant of capillary pressures, which only enters at higher order.

We now discuss briefly how the result in (11) fits together with the physical interpretation of attraction and repulsion that we developed in section II. Running through the calculation outlined above for spheres that are not identical, the reader will see that the sign of the interaction force is determined by the sign of $z'_c{}^{(1)} \sin \phi_c{}^{(1)} \times z'_c{}^{(2)} \sin \phi_c{}^{(2)}$, where the superscript (i) labels the two particles: the interaction is attractive if this product is positive and repulsive if it is negative. From (9) this product has the same sign as the product of the gradients of the two interfaces in the neighbourhood of the two particles, and so we see that there is mutual attraction if the particles have like menisci and repulsion if they have unlike menisci. This is precisely the picture that we saw in section II, although we are now able to quantify the combination of contact angles and particle densities that give rise to the two different possibilities. We also note that the strength of the interaction

decreases as the surface tension coefficient, γ , increases. This slightly counterintuitive result is actually a simple consequence of the fact that for higher values of γ the deformation of the interface required to satisfy the vertical force balance condition for particle 1 is less and so the gravitational hill upon which particle 2 finds itself is smaller.

VI. THE DYNAMICS OF FLOATING PARTICLES

Previously, we have focused exclusively on the static properties of various objects at a liquid-gas interface. When calculating the force of interaction, we have in fact been calculating the horizontal force that would be required to keep those objects a fixed distance apart. We shall now turn our attention to understanding this interaction dynamically and answer some questions that arise naturally from observing the motion of objects at an interface. Perhaps the most natural question to start with is "how fast do two spherical particles come together?" and it is this that we shall focus on in this section.

To make the dynamical problem tractable, we assume that the vertical velocity of each particle as it moves along the meniscus is small enough that the vertical force balance used to determine the horizontal force is satisfied; an assumption that is valid to higher order in B as shown by Chan *et al.*⁸. Another question arises as to how to incorporate dynamics into this problem. One possibility is that adopted by Chan *et al.*⁸ who neglect the influence of the fluid altogether and assume instead that the particle moves ballistically under the action of the interaction force. Instead of adopting this approach, we assume that the motion is overdamped so that a Stokes drag term⁴ (for the viscous drag provided by the liquid) balances the attractive force between the two particles given in (11). This balance may be written as:

$$6\pi\mu R\alpha \frac{dl}{dt} = -2\pi\gamma R B^{5/2} \Sigma^2 K_1 \left(\frac{l(t)}{L_c} \right) \quad (12)$$

where μ is the dynamic viscosity of the liquid and α is a scaling factor to take into account the fact that the drag experienced by a particle at an interface is less than it would experience if completely immersed in the bulk fluid. Here, we take $\alpha = 1/2$ for simplicity although Danov *et al.*¹² computed numerically the dependence of α on θ . Data obtained from observing two spherical particles with radius 0.3 mm as they move under each other's influence is shown in fig. 8. Here the value of Σ is difficult to measure experimentally because of its dependence on the contact angle θ and so we use Σ as a parameter to fit the experimental data to the numerical solution of (12).

In this case, we are assuming that the particles are sufficiently small that their inertia may be neglected entirely. In fact, the approach we have adopted is better suited to such small particles since the Bond number in this situation is also very small and so the expression for

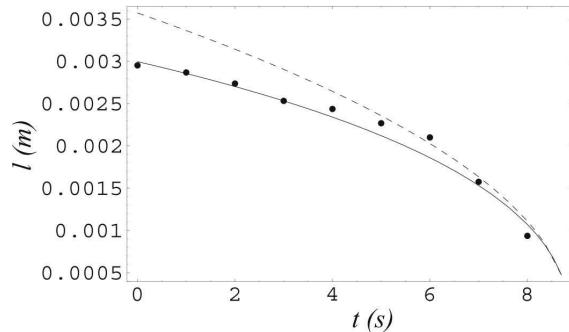


FIG. 8: Experimental data (points) compared to the model (solid line) for two identical spheres of radius 0.3mm interacting via flotation forces at an air-water interface. The theoretical curve is calculated from the model with $\gamma = 0.0728 \text{ Nm}^{-1}$ and $\mu = 0.001 \text{ Pa s}$ with $\Sigma = 0.58$ used as a fitting parameter. The dashed line gives the asymptotic result (13).

the interaction force in (11) is effectively exact. Also, if the typical distance between particles is small (compared to the capillary length, L_c) then we are again able to use the asymptotic formula $K_1(x) \approx x^{-1}$ for $x \ll 1$ to approximate the modified Bessel function that occurs in the force-law (11). Substituting this into (12) allows us to solve for $l(t)$, giving:

$$l(t) \approx \sqrt{l(0)^2 - \frac{2\gamma L_c B^{5/2} \Sigma^2}{3\mu\alpha} t} \quad (13)$$

so that the time taken for two spheres to come into contact is given by:

$$t_{\text{contact}} \approx \frac{3\mu\alpha(l(0)^2 - R^2)}{2\gamma L_c B^{5/2} \Sigma^2} \quad (14)$$

It is also possible to perform a consistency check of our assumption that the motion is slow enough for our neglect of the particle's acceleration to be valid. To do this, it is enough to check that the ratio of particle inertia to Stokes drag, \mathcal{R} , is small as the particles come into contact as the value of \mathcal{R} is greatest at this point. Using the asymptotic expression for $K_1(x)$, we have:

$$\mathcal{R}_{\text{contact}} = \frac{2}{27\alpha^2} \frac{\gamma\rho L_c B^{5/2} \Sigma^2}{3\mu^2} \quad (15)$$

Using this result, it is simple to show that for spherical particles of radius less than 0.3mm (or $B = 0.01$), $\mathcal{R} < 0.1$ throughout the motion, which is sufficiently small that our approach is self-consistent.

VII. AMPHIPHILIC STRIPS WITHOUT CHEMISTRY

As a final illustration of the principles that we have applied to the problem of the attraction of interfacial objects we shall consider briefly the equilibrium of a single

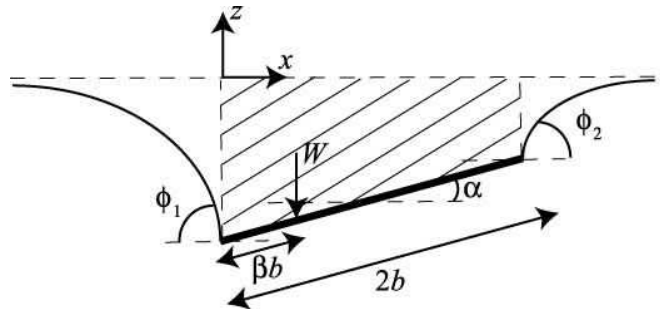


FIG. 9: A single two-dimensional strip (of weight W per unit length in the direction perpendicular to the page) floating at an interface, with the hatched area indicating the area of displaced fluid the weight of which is equal to the buoyancy force on the strip. The asymmetric equilibrium position here is possible because of an off-centre position for the strip's centre of mass.

strip (of weight W per unit length) floating horizontally at an interface, as shown in fig. 9. This problem was studied extensively by Mansfield *et al.*¹⁰ who also investigated the interactions between two such strips. Here, however, we content ourselves with studying the simpler problem with a single strip but with a slight twist: we take the centre of mass line of the strip to be displaced from the strip's centre line by a distance $(1 - \beta)b$. As we shall see, this is enough to break the symmetry of the problem and thus allow the strip to float at an angle α to the horizontal.

Because the strip is assumed to be infinitely thin, the concept of contact angle that we met earlier is not well-defined in this problem. Instead, the effective contact angles that the interface makes at the points of contact with the strip, $\phi_{1,2}$, and the angle α are determined from the condition that the strip be in equilibrium, which leads to three equations for the three unknowns. The first two of these are the conditions of horizontal and vertical force balance, which we have encountered previously and here may be written:

$$0 = \gamma(\cos \phi_1 - \cos \phi_2) + \frac{\rho g}{2}(z_1^2 - z_2^2) \quad (16)$$

for horizontal equilibrium and:

$$W = \gamma(\sin \phi_1 + \sin \phi_2) - \rho g(2b \cos \alpha) \left(\frac{z_1 + z_2}{2} \right) \quad (17)$$

for vertical equilibrium - the second term on the right hand side in (17) simply being the weight of liquid displaced by the strip, which is shown as the hatched area in fig. 9. In addition, there is the condition of torque balance, which we did not encounter for the equilibrium of the floating sphere (it is automatically satisfied for objects of circular cross-section). Here, however, this condition is crucial as it gives a third equation by which to determine the three unknowns. By taking moments

about the centre of mass, we have:

$$0 = \gamma b ((2 - \beta) \sin(\phi_2 - \alpha) - \beta \sin(\phi_1 + \alpha)) - \rho g \int_{-\beta b}^{(2-\beta)b} z(s) s ds \quad (18)$$

where s is an arc-length co-ordinate measured along the strip from the centre of mass.

In principle, these equations can be solved even for interfacial deformations that are not small following the strategy outlined by Mansfield *et al.*¹⁰. However, for simplicity, we proceed here in the limit where the three angles are small and, therefore, the interfacial deformations are also small. In this limit, we have that $z_{1,2} \approx -L_c \phi_{1,2}$ and so the vertical relation (17) becomes simply:

$$\frac{W}{\gamma} = (\phi_1 + \phi_2) \left(1 + \frac{b}{L_c} \right) \quad (19)$$

Also, the linearised version of (16) is automatically satisfied and so we make use of the geometrical relation $z_2 - z_1 = 2b \sin \alpha$ to give:

$$\alpha = \frac{\phi_1 - \phi_2}{2b/L_c} \quad (20)$$

Finally, the torque balance condition (18) yields:

$$0 = (2 - \beta)\phi_2 - \beta\phi_1 - 2\alpha + \frac{b}{L_c}(1 - \beta)(\beta\phi_2 + (2 - \beta)\phi_1) + \frac{b}{L_c} \frac{\phi_2 - \phi_1}{6} (\beta^3 + (2 - \beta)^3) \quad (21)$$

Together, equations (19)-(21) constitute a system of three linear equations in three unknowns, which can be solved simply by inverting a 3×3 matrix. Of particular interest here is the possibility that, for some values of β , we may have ϕ_1 and ϕ_2 of opposite sign and so plotted in fig. 10 is the dependence of $\phi_1\phi_2$ on β showing that for sufficiently small β , ϕ_1 and ϕ_2 are of opposite sign. We can understand this more fully by solving the system (19)-(21) to give:

$$\phi_1\phi_2 = \frac{W^2}{\gamma^2} L_c^2 \frac{(3L_c^2 + 6bL_c + 4b^2 - 3b(L_c + b)\beta)(3L_c^2 - 2b^2 + 3b(L_c + b)\beta)}{4(L_c + b)^2(b^2 + 3bL_c + 3L_c^2)^2} \quad (22)$$

From this and the restriction that $\beta \leq 1$, it is a simple matter to show that $\phi_1\phi_2 < 0$ when $\beta < \frac{2b^2 - 3L_c^2}{3b(b + L_c)}$ and hence that ϕ_1 and ϕ_2 are of opposite sign for sufficiently small β provided that $b > (3/2)^{1/2}L_c$.

The significance of $\phi_1\phi_2 < 0$ is that in such cases the two edges of the strip have fundamentally different interface shapes associated with them: one edge is able to attract drawing pins while the other repels drawing pins and attracts bubbles instead! Particles or molecules with this type of behaviour are often termed *amphiphiles* and occur in detergents along with many other applications¹³. However, such amphiphilic particles are usually constructed by treating the two edges chemically to induce the very different behaviour: here, we have shown that this may also be achieved by altering the density of the strip so that the centre of mass of the object is displaced.

As well as the possible industrial applications that particles such as this could have, this *physical* amphiphile lends itself to a much simpler classroom demonstration than might be possible with chemical amphiphiles. Using a piece of sticky tape doubled back on itself to form the strip, see fig. 11 (a), and a short length of wire (part of a paperclip for example) inserted between the two sides

of tape, it is possible to make a strip with edges that deform the interface in manifestly different ways. An experimental realisation of this is shown in fig. 11 (b), which demonstrates that such particles are an effective means by which particles that would otherwise be mutually repulsive can be coaxed into maintaining a finite equilibrium separation.

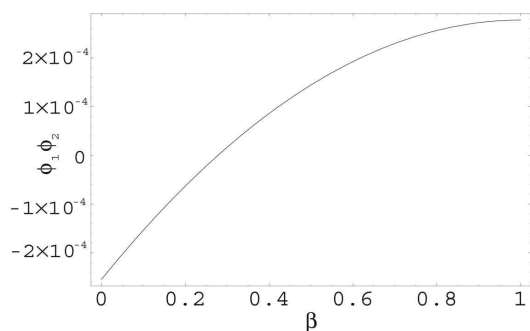


FIG. 10: The dependence of $\phi_1\phi_2$ on $\beta \in [0, 1]$ (the graph being symmetric about $\beta = 1$). Here $W/\gamma = 0.1$ and $b/L_c = 2$.

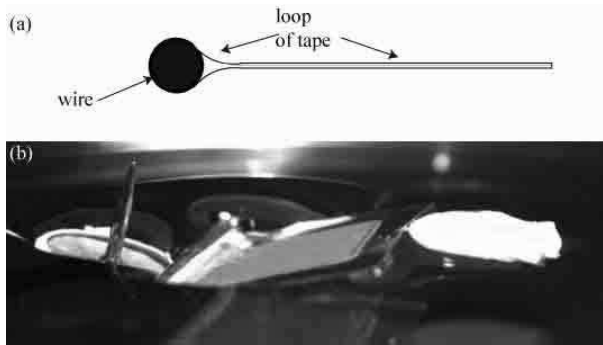


FIG. 11: Example of a simple amphiphilic strip. (a) Simple design of the amphiphilic strip mentioned in the text. (b) Photograph of such an amphiphilic strip bonding a drawing pin (left) and the cap of another drawing pin (right), which would normally be mutually repulsive. Using such an amphiphile allows particles that would otherwise be repulsive to be maintained stably at an almost arbitrary separation.



FIG. 12: The interfacial deformation caused by a water-spider. Here, the meniscus is visibly depressed by the spider's weight acting on each leg (<http://faculty.vassar.edu/suter/1websites/sutersite/Locomotion/images.htm>).

VIII. DISCUSSION

In this article we have investigated an aspect of everyday life that may previously have escaped our readers' notice - the propensity of floating objects to aggregate. Having couched the mechanism for this effect in terms of the simple physics of particles trapped at a deformed interface feeling the effects of their weight (or buoyancy), we have shown how approximate methods can lead to quantitative descriptions of the magnitude of the interaction 'force' and the dynamical nature of the interaction. We now conclude with a brief discussion of some of the scenarios in which this effect has found application and point out some potential research directions.

As is often the case, the first place to look after obtaining a better understanding of a novel physical idea is mother nature. Doubtless there are many instances

where a variant of the Cheerios effect is used by some species or another. Here, however, we choose to highlight one particular application in the natural world: water walking creatures that can be found on the surface of many ponds. Many of these animals rely on surface tension to prevent them from drowning as their weight can be supported by interfacial deformations (as is shown in fig. 12). While this interfacial phenomenon should be welcomed by such creatures, they become reluctant victims of the Cheerios effect whenever they try to climb out of the pond, since this generally requires climbing up the meniscus - against gravity. Recent observations by David Hu and John Bush¹⁴ suggest that some insects such as *Mniovelgia Kuscheli* may pull up on the meniscus with their front legs and push down on it with their hind legs, thus becoming the natural exemplar of the amphiphile discussed in the last section. Having first been thwarted by the Cheerios effect, they have the last laugh by using it to hitch a ride up the meniscus!

Currently, mankind's efforts at making use of the Cheerios effect are not quite as developed as nature's. Much attention has been focused on using surface tension effects to assemble ordered arrays of particles² with a view to eventually forming intricate, structured aggregates of small components in a controlled manner. The aim is to understand the interactions between floating objects to the point where it is possible to float a series of components on a layer of water and wait while they 'self-assemble' into some larger structure. Once this has happened, the layer of water could be evaporated leaving the components in their original form and able to be used as a micro-device. Presently, such applications are a long way off but have taken a step closer to reality after detailed investigation of the interactions between floating objects and ways in which the strength of interaction and even its direction may be tuned.

There remain many interesting questions that we have not been able to answer in this article, many of which are certainly amenable to investigation in the classroom or the laboratory. For example, the motion of a flexible filament induced by surface tension has yet to be studied either experimentally or theoretically. It would also be worthwhile to better understand the way in which two different types of particles that are mutually repulsive interact. With a mixture of light and heavy particles, for example, clusters of like density particles form - all things (other than the particle density) being equal. This segregation phenomenon would undoubtedly find many applications within science and industry. Such a study could then naturally be extended by the inclusion of amphiphilic particles, which would allow the user to dictate a finite equilibrium spacing between two otherwise repulsive objects. The inspiration from nature and industry seems almost overwhelming.

Acknowledgments

This article arose as a result of a summer studentship funded by the Heilbronn Fund of Trinity College, Cam-

bridge (D.V.). We thank John Bush and David Hu for telling us about the meniscus-climbing insect *Mniodelia Kuscheli*, and Pascale Aussillous for assistance with the photography in figures 1, 3 and 11 (b).

* Electronic address: lm@deas.harvard.edu

¹ J. Walker, *The Flying Circus of Physics*, (Wiley, 1977).

² G. M. Whitesides and B. Grzybowski, “Self-assembly at all scales”, *Science* **295**, 2418-2421 (2002).

³ M. M. Nicolson, “The interaction between floating particles”, *Proc. Camb. Philos. Soc.* **45**, 288-295 (1949).

⁴ G. K. Batchelor, *An Introduction to Fluid Dynamics* (Cambridge University Press, Cambridge, 1967).

⁵ D. J. Campbell, E. R. Freidinger, J. M. Hastings and M. K. Querns, “Spontaneous assembly of soda straws”, *J. Chem. Educ.* **79**, 201-202 (2002).

⁶ J. C. Maxwell, “Capillary action”, in *The Scientific Papers of James Clerk Maxwell* vol. 2, Ed. W. D. Niven (Cambridge University Press, Cambridge, 1890).

⁷ J. H. Poynting and Sir J. J. Thomson, *A Text-Book of Physics: Volume I (Properties of Matter)*, (Griffin Co., 1913).

⁸ D. Y. C. Chan, J. D. Henry Jr. and L. R. White, “The interaction of colloidal particles collected at a fluid inter-

face”, *J. Colloid Interface Sci.* **79**, 410-418 (1981).

⁹ J. B. Keller, “Surface tension force on a partly submerged body”, *Phys. Fluids* **10**, 3009-1010 (1998).

¹⁰ E. H. Mansfield, H. R. Sepangi and E. A. Eastwood, “Equilibrium and mutual attraction or repulsion of objects supported by surface tension”, *Phil. Trans. R. Soc. Lond. A* **355**, 869-919 (1997).

¹¹ M. Abramowitz and I. A. Stegun, *Handbook of Mathematical Functions* (Dover, New York, 1965).

¹² K. D. Danov, R. Dimova and B. Pouligny, “Viscous drag of a solid sphere straddling a spherical or flat interface”, *Phys. Fluids* **12**, 2711-2722 (2000).

¹³ T. Ondarçuhu, P. Fabre, E. Raphaël and M. Veysié, “Specific properties of amphiphilic particles at fluid interfaces”, *J. Phys. Paris* **51**, 1527-1536 (1990).

¹⁴ David Hu’s website has some movies showing *Mniodelia Kuscheli* performing this trick:
<http://www-math.mit.edu/~dhu/Videoweb/2top.mov>